Instabilities of wormholes and regular black holes supported by a phantom scalar field

K. A. Bronnikov*

Center for Gravitation and Fundamental Metrology, VNIIMS, Ozyornaya 46, Moscow 119361, Russia; and Institute of Gravitation and Cosmology, PFUR, ul. Miklukho-Maklaya 6, Moscow 117198, Russia

R. A. Konoplya†

DAMTP, Centre for Mathematical Sciences, University of Cambridge, Wilberforce Road, Cambridge CB3 0WA, United Kingdom; and Centro de Estudios Científicos (CECS), Casilla 1469, Valdivia, Chile

A. Zhidenko‡

Centro de Matemática, Computação e Cognição, Universidade Federal do ABC (UFABC), Rua Santa Adélia, 166, 09210-170, Santo André, SP, Brazil

(Received 11 May 2012; published 18 July 2012)

We test the stability of various wormholes and black holes supported by a scalar field with a negative kinetic term. The general axial perturbations and the monopole type of polar perturbations are considered in the linear approximation. Two classes of objects are considered: (i) wormholes with flat asymptotic behavior at one end and anti-de Sitter on the other (Minkowski–anti-de Sitter wormholes) and (ii) regular black holes with asymptotically de Sitter expansion far beyond the horizon (the so-called black universes). A difficulty in such stability studies is that the effective potential for perturbations forms an infinite wall at throats, if any. Its regularization is in general possible only by numerical methods, and such a method is suggested in a general form and used in the present paper. As a result, we have shown that all configurations under study are unstable under spherically symmetric perturbations, except for a special class of black universes where the event horizon coincides with the minimum of the area function. For this stable family, the frequencies of quasinormal modes of axial perturbations are calculated.

DOI: 10.1103/PhysRevD.86.024028 PACS numbers: 04.70.Bw, 04.50.Kd, 04.20.Jb

I. INTRODUCTION

Modern observations [1] indicate that the Universe is expanding with acceleration. The most favored explanation of this acceleration is nowadays that the Universe is dominated (to about 70%) by some unknown form of energy density with large negative pressure, termed dark energy (DE), while the remaining 30% consisting of baryonic and nonbaryonic visible and dark matter. It is often admitted that DE can be modeled by a self-interacting scalar field with a potential. Such a field acts as a negative pressure source; it is called quintessence if its pressure to density ratio $p/\rho = w > -1$ and a phantom field if $w < -1$ while $w = -1$ corresponds to a cosmological constant Λ. Since observations admit a range of w including $w = -1$, all sorts of models are under study.

One should note that values $w < -1$ seem to be not only admissible but even preferable for describing an increasing acceleration, as follows from the most recent estimates: $w = -1.10 \pm 0.14$ (1σ) [2] (according to the 7-year WMAP data) and $w = -1.069^{+0.091}_{-0.092}$ [3] (mainly from data on type Ia supernovae from the SNLS3 sample). In this connection, cosmological models with phantom scalar fields, i.e., those with a negative kinetic term, have gained considerable attention in the recent years [4].

If such fields can play an important role in cosmology, it is natural to expect that they manifest themselves in local phenomena, for instance, in the existence and properties of black holes and wormholes [5]. Quite a number of scalar field configurations of this kind have been described in the literature, see, e.g., examples of black holes with scalar fields (the so-called scalar hair) in [6] and wormholes supported by scalar fields in [7–9] and references therein. Thus, in [9] it was shown that, in addition to wormholes, a phantom scalar can support a regular black hole where a possible explorer, after crossing the event horizon, gets into an expanding universe instead of a singularity. Thus such hypothetical configurations combine the properties of a wormhole (absence of a center, a regular minimum of the area function) and a black hole (a Killing horizon separating R and T regions). Moreover, the Kantowski-Sachs cosmology that occurs in the T region is asymptotically isotropic and approaches a de Sitter regime of expansion, which makes such models potentially viable as models of our accelerating Universe. Such configurations, termed *black universes,* were later shown to exist with other scalar field sources exhibiting a phantom behavior such as k-essence [10] and some brane world models [11] (in the latter case, even without a phantom field).

*kb20@yandex.ru
†konoplya_roma@yahoo.com
‡olexandr.zhydenko@ufabc.edu.br

Both wormholes and black universes have been shown to exist as well in models where a scalar field exhibits phantom properties only in a strong-field region while in the weak-field region it obeys the canonical field equation (the so-called *trapped-ghost models*) [12,13].

To see whether or not such solutions can lead to viable models of black holes and wormholes, one needs to check their stability against various perturbations. Previously, gravitational stability as well as passage of radiation through wormholes supported by a phantom scalar field were considered, in particular, in [14–18], with a special emphasis on massless wormholes (see also references therein).

In the present paper, we consider the linear stability of various static, spherically symmetric solutions to the field equations of general relativity with minimally coupled scalar fields, describing compact objects of interest such as asymptotically flat and AdS wormholes (M-AdS wormholes, for short, where M stands for "Minkowski") and black universes (in other words, M-dS regular black holes), and use as examples solutions obtained in [9]. We show that M-AdS wormholes are unstable in the whole range of the parameters while among black universes there is a stable subfamily which corresponds to the event horizon located precisely at the minimum of the area function.

The particular solutions whose stability is studied here are certainly not general. A more comprehensive study is prevented by the fact that a sufficiently general solution describing self-gravitating scalar fields with nonzero potentials is unknown, therefore it seems to be a natural decision to study the properties of known special solutions. On the other hand, in [9] all possible regular static, spherically symmetric solutions to the field equations were classified for phantom minimally coupled scalar fields with arbitrary potentials. One can see that the solution studied here, being certainly special, still represents a very simple but quite typical example reproducing the generic features of such configurations with flat, dS and AdS asymptotics; its other advantage is that it reproduces as a special case the well-known Ellis wormhole, for which the stability results are already known [14–16].

The paper is organized as follows. Section II presents the backgrounds to be considered. Section III develops a general formalism for axial gravitational and Maxwell field perturbations in a static, spherically symmetric background. Section IV is devoted to polar spherically symmetric perturbations. Section V discusses the stability of the black universes and wormholes under consideration and analyzes the quasinormal radiation spectrum for the cases where the background configuration is linearly stable. In addition, we then develop a numerical tool for reducing the wavelike equation with a singular potential to the one with a regular potential. In Sec. VI we summarize the results and mention some open problems.

II. STATIC BACKGROUND CONFIGURATIONS

Let us consider Lagrangians of the form

$$L = \sqrt{-g}(R + \epsilon g^{\alpha\beta}\phi_{;\alpha}\phi_{;\beta} - 2V(\phi) - F_{\mu\nu}F^{\mu\nu}), \quad (1)$$

which includes a scalar field, in general, with some potential $V(\phi)$, and an electromagnetic field $F_{\mu\nu}$; $\epsilon = \pm 1$ distinguishes normal, canonical scalar fields ($\epsilon = +1$) and phantom fields ($\epsilon = -1$). In what follows, we present a perturbation analysis for static, spherically symmetric solutions for this general type of Lagrangian and then study the stability of some particular (electrically neutral) solutions.

The general static, spherically symmetric metric can be written in the form

$$ds^2 = A(r)dt^2 - A(r)^{-1}dr^2 - R(r)^2 d\Omega^2, \quad (2)$$

where $d\Omega^2 = d\theta^2 + \sin^2\theta d\varphi^2$ is the linear element on a unit sphere.

We will consider the following static background [9]:

$$\begin{aligned} R(r) &= (r^2+b^2)^{1/2}, \qquad b = \text{const} > 0, \\ A(r) &= (r^2+b^2) \\ &\quad \times \left[\frac{c}{b^2} + \frac{1}{b^2+r^2} + \frac{3m}{b^3}\left(\frac{br}{b^2+r^2} + \tan^{-1}\frac{r}{b}\right)\right], \\ \phi &= \sqrt{2}\tan^{-1}(r/b). \end{aligned} \quad (3)$$

It is a solution to the Einstein-scalar equations that follow from (1) with $F_{\mu\nu} \equiv 0$ and the potential

$$V(\phi) = -\frac{c}{b^2}\left[3 - 2\cos^2\left(\frac{\phi}{\sqrt{2}}\right)\right] - \frac{3m}{b^3}\left[3\sin\frac{\phi}{\sqrt{2}}\cos\frac{\phi}{\sqrt{2}} + \frac{\phi}{\sqrt{2}}\left(3 - 2\cos^2\frac{\phi}{\sqrt{2}}\right)\right]. \quad (4)$$

The solution behavior is controlled by the scale b and two integration constants: c that moves the curve $B(r) \equiv A/R^2$ up and down, and m showing the position of the maximum of $B(r)$. Both $R(r)$ and $B(r)$ are even functions if $m = 0$, otherwise $B(r)$ loses this symmetry. Asymptotic flatness at $r = +\infty$ implies

$$2bc = -3\pi m, \quad (5)$$

where m is the Schwarzschild mass defined in the usual way.

Under this asymptotic flatness assumption, for $m = c = 0$, we obtain the simplest symmetric configuration, the Ellis wormhole [7]: $A \equiv 1$, $V \equiv 0$. With $m < 0$, we obtain a wormhole with an AdS metric at the far end, corresponding to the cosmological constant $V(\phi)|_{r\to-\infty} = V_- < 0$. Further on, such configurations will be referred to as M-AdS wormholes (where M stands for Minkowski, the flat asymptotic). Assuming $m > 0$, at large negative r we obtain negative $A(r)$, such that $|A(r)| \sim R^2(r)$, and a potential tending to $V_- > 0$. Thus it is a regular black hole with a de Sitter asymptotic behavior far beyond the horizon, precisely corresponding to the above description of a black universe.

In black universe solutions, the horizon radius depends on both parameters m and b ($\min R(r) = b$), which also plays the role of a scalar charge since $\phi/\sqrt{2} \approx \pi/2 - b/r$ at large r. Since $A(0) = 1 + c$, the minimum of $R(r)$, located at $r = 0$, occurs in the R region if $c > -1$, i.e., if $3\pi m < 2b$ (it is then a throat, like that in wormholes), right at the horizon if $c = -1$ (i.e., $3\pi m = 2b$) and in the T region beyond it if $c < -1$, that is, $3\pi m > 2b$. It is then not a throat, since r is a time coordinate, but a bounce in one of the scale factors $R(r)$ of the Kantowski-Sachs cosmology; the other scale factor is $A(r)$.

Let us mention that another important case of the system (1), the one with $V \equiv 0$, has already been studied in a number of papers. In this case we are dealing with Fisher's famous solution ([19], 1948) for a canonical massless scalar in general relativity ($\epsilon = +1$) and three branches of its counterpart for $\epsilon = -1$, sometimes called the anti-Fisher solution, found for the first time by Bergmann and Leipnik [20] in 1957 and repeatedly rediscovered afterwards (as well as Fisher's solution). In the latter case the solution consists of three branches, one representing wormholes [7,8], the other two also containing throats but with singularities or horizons of infinite area at the far end instead of another spatial infinity [8,21]. An instability of Fisher's solution under spherically symmetric perturbations was established long ago [22], a similar instability of the wormhole branch was discovered in [14,16] and the same for the other two branches in [23]. The case of zero mass in the anti-Fisher solution represents the Ellis wormhole and is common with the solution under study, (3), $m = 0$.

In what follows, we will assume $m \neq 0$ and use the mass m (which has the dimension of length and is equal to half the Schwarzschild radius in the units employed) as a natural length scale, putting, for convenience, $|3m| = 1$. Then the constant c is used as a family parameter while b is found from the relation (5).

We should remark that in all particular examples to be tested here for stability the background electromagnetic field is zero, but the general perturbation formalism is developed in Sec. III for axial perturbations of systems with nonzero $F_{\mu\nu}$ as well. Actually in Sec. IV nonzero $F_{\mu\nu}$ is also allowed, simply because the monopole perturbations do not excite an electromagnetic field in a spherically symmetric background. Perturbations of the electromagnetic field appear in higher multipoles of polar modes. The general formalism developed for nonzero $F_{\mu\nu}$ is intended to be used in further studies of systems with both scalar and electromagnetic fields.

III. LINEAR AXIAL PERTURBATIONS: GENERAL ANALYSIS

In our analysis of axial perturbations, we use Chandrasekhar's notations: $x^0 = t$, $x^1 = \phi$, $x^2 = r$, $x^3 = \theta$, so that the coordinates along which the background has Killing vectors are enumerated first. Following Chandrasekhar [24], we consider the metric (2) as a special case of the metric

$$ds^2 = e^{2\nu}dt^2 - e^{2\psi}(d\phi - \sigma dt - q_2 dr - q_3 d\theta)^2 - e^{2\mu_2}dr^2 - e^{2\mu_3}d\theta^2. \quad (6)$$

Thus in (2)

$$e^{2\nu} = A(r), \qquad e^{2\mu_2} = A^{-1}(r), \qquad e^{2\mu_3} = R(r)^2, \qquad e^{2\psi} = R(r)^2 \sin^2\theta. \quad (7)$$

The background electromagnetic field is taken in the form

$$F_{02} = -Q_*/R(r)^2, \quad (8)$$

that is, only a radial electric field, and Q_* is the (effective) charge.

All calculations and results can be easily rewritten for magnetic fields, with nonzero F_{13}, owing to the Maxwell field duality. One can bear in mind that configurations like wormholes and black universes can possess electric or magnetic fields without any real electric charges or magnetic monopoles, due to their geometry, actually realizing Wheeler's concept of a "charge without charge".

It is easy to see that axial perturbations of a scalar field vanish. Then, σ, q_2 and q_3 are perturbed, while ψ, μ_2, μ_3 and ν remain unperturbed.

The axial gravitational perturbations obey the equations

$$\delta R_{13} = 0, \qquad \delta R_{12} = 2Q_* R^{-2} F_{01}. \quad (9)$$

Let us introduce new variables:

$$Q_{ik} = q_{i,k} - q_{k,i}, \qquad Q_{i0} = q_{i,0} - \sigma_{,i}, \quad (10)$$

with $i, k = 2, 3$, and

$$E \equiv F_{01} \sin\theta. \quad (11)$$

Recall that we use the numbers 0, 1, 2, 3 for t, ϕ, r and θ coordinates, respectively. The Maxwell equations, subject to only first-order perturbations, have the form

$$(e^{\psi+\mu_2}F_{12})_{,3} + (e^{\psi+\mu_3}F_{31})_{,2} = 0, \quad (12)$$

$$(e^{\psi+\nu}F_{01})_{,2} + (e^{\psi+\mu_2}F_{12})_{,0} = 0, \quad (13)$$

$$(e^{\psi+\nu}F_{01})_{,3} + (e^{\psi+\mu_3}F_{13})_{,0} = 0, \quad (14)$$

$$(e^{\mu_2+\mu_3}F_{01})_{,0} + (e^{\nu+\mu_3}F_{12})_{,2} + (e^{\nu+\mu_2}F_{13})_{,3} = e^{\psi+\mu_3}F_{02}Q_{02}. \quad (15)$$

After some algebra the Maxwell equations can be written in the form

$$Re^{-\nu}E_{,0,0} - (e^{2\nu}(Re^{\nu}E)_{,r})_{,r} + \frac{e^{\nu}}{R}\sin\theta\left(E_{,\theta}\frac{1}{\sin\theta}\right)_{,\theta} = -Q_*(\sigma_{,2,0} - q_{2,0,0})\sin^2\theta. \quad (16)$$

From $\delta R_{13} = 0$ and $\delta R_{12} = 2Q_* R^{-2} F_{01}$ it follows

$$(e^{3\psi+\nu-\mu_2-\mu_3} Q_{23})_{,2} - (e^{3\psi-\nu+\mu_2-\mu_3} Q_{03})_{,0} = 0 \qquad (17)$$

and

$$(e^{3\psi+\nu-\mu_2-\mu_3} Q_{23})_{,3} - (e^{3\psi-\nu-\mu_2+\mu_3} Q_{02})_{,0} = e^{2\psi+\nu+\mu_3} Q_* R^{-2} F_{01}. \qquad (18)$$

After introducing the new function

$$Q \equiv R^2 A Q_{23} \sin^3\theta, \qquad (19)$$

Eqs. (17) and (18) can be written in the form

$$\frac{A}{R^2 \sin^3\theta} \frac{\partial Q}{\partial r} = \sigma_{,3,0} - q_{3,0,0}, \qquad (20)$$

$$\frac{A}{R^4 \sin^3\theta} \frac{\partial Q}{\partial \theta} = -\sigma_{,2,0} + q_{2,0,0} + \frac{4Q_* e^\nu E}{R^2 \sin^2\theta}. \qquad (21)$$

Let us differentiate Eq. (20) in r and Eq. (21) in θ and then add the results. After some algebra we have

$$R^4 \frac{\partial}{\partial r}\left(\frac{A}{R^2}\frac{\partial Q}{\partial r}\right) + \sin^3\theta \frac{\partial}{\partial \theta}\left(\frac{1}{\sin^3\theta}\frac{\partial Q}{\partial \theta}\right) - \ddot{Q} R^2 e^{-2\nu} = 4Q_* e^\nu R \sin^3\theta \frac{\partial}{\partial\theta}\left(\frac{E}{\sin^2\theta}\right). \qquad (22)$$

Now let us return to the Maxwell field perturbation equation (16). Using (21), we can get rid of the term containing $\sigma_{,2,0} - q_{2,0,0}$ in (10). After some algebra and using the relations $E \sim e^{i\omega t}$, $Q \sim e^{i\omega t}$, we obtain

$$(e^{2\nu}(Re^\nu E)_{,r})_{,r} + E(\omega^2 R e^{-\nu} - 4Q_*^2 e^\nu R^{-3}) - e^\nu R^{-1} \sin\theta \left(E_{,\theta} \frac{1}{\sin\theta}\right)_{,\theta} = -\frac{Q_*}{R^4 \sin\theta}\frac{\partial Q}{\partial \theta}. \qquad (23)$$

The angular variable can be separated by the following ansatz:

$$Q(r,\theta) = Q(r) C_{\ell+2}^{-3/2}(\theta), \qquad (24)$$

$$E(r,\theta) = \frac{E(r)}{\sin\theta}\frac{dC_{\ell+2}^{-3/2}(\theta)}{d\theta} = 3E(r) C_{\ell+1}^{-1/2}(\theta), \qquad (25)$$

where C_a^b are Gegenbauer polynomials. Eqs. (22) and (23) then read

$$\Delta \frac{d}{dr}\left(\frac{\Delta}{R^4}\frac{dQ}{dr}\right) - \mu^2 \frac{\Delta}{R^4} Q + \omega^2 Q = -\frac{4Q_* \mu^2 \Delta e^\nu E}{R^3}, \qquad (26)$$

$$(e^{2\nu}(Re^\nu E)_{,r})_{,r} - (\mu^2 + 2) e^\nu R^{-1} E + E(\omega^2 R e^{-\nu} - 4Q_*^2 e^\nu R^{-3}) = -Q_* Q R^{-4}, \qquad (27)$$

where $\Delta = R^2 e^{2\nu}$, $\mu^2 = (\ell - 1)(\ell + 2)$, and we use the tortoise coordinate r_* defined by $d/dr_* = \Delta R^{-2} d/dr$.

After passing over from Q and E to the new functions H_1 and H_2 using the relations

$$Q = RH_2, \qquad Re^\nu E = -\frac{H_1}{2\mu}, \qquad (28)$$

Eqs. (26) and (27) can be reduced to

$$\Lambda^2 H_2 = \left(\frac{R_{,r_* r_*}}{R} - \frac{2R_{,r_*}^2}{R^2} - \mu^2 \frac{\Delta}{R^4}\right) H_2 - \frac{2Q_* \mu \Delta}{R^5} H_1, \qquad (29)$$

$$\Lambda^2 H_1 = \frac{\Delta}{R^4}\left((\mu^2 + 2) - \frac{4Q_*^2}{R^2}\right) H_1 - 2Q_* \mu H_2, \qquad (30)$$

where we have introduced the operator

$$\Lambda^2 = \frac{d^2}{dr_*^2} + \omega^2. \qquad (31)$$

For an electrically neutral background $Q_* = 0$, $H_1 = 0$, and Eq. (29) reduces to the Schrödinger-like equation

$$\frac{d^2 H_2}{dr_*^2} + (\omega^2 - V_{\rm eff}(r)) H_2 = 0, \qquad (32)$$

with the effective potential

$$V_{\rm eff}(r) = A(r)\frac{(\ell + 2)(\ell - 1)}{R^2} + R(R^{-1})_{,r_*,r_*}. \qquad (33)$$

As a partial verification of the above relations, we can check that Eqs. (29) and (30) reproduce some known special cases. Thus, Eq. (33), obtained here in the Chandrasekhar approach [24], coincides with Eq. (4.13) of [25], obtained in the Regge-Wheeler approach. In addition, Eqs. (29) and (30) coincide with Eqs. (144) and (145), p. 230 of [24] in the Reissner-Nordström limit, and, as a result, the potential (33) coincides with the well-known Regge-Wheeler potential for Schwarzschild black holes.

IV. POLAR PERTURBATIONS

For polar perturbations let us consider the Einstein-scalar equations following from (1) with $F_{\mu\nu} = 0$

$$R_{\mu\nu} + \epsilon \partial_\mu \Phi \partial_\nu \Phi - \delta_{\mu\nu} V(\phi) = 0, \quad \epsilon \Box \Phi + V_\phi = 0, \quad V_\phi \equiv dV/d\phi, \qquad (34)$$

where $\Box = \nabla^\alpha \nabla_\alpha$ is the d'Alembert operator. In the polar case we can put $\sigma = q_2 = q_3 = 0$, while $\delta\nu$, $\delta\mu_2$, $\delta\mu_3$, and $\delta\psi$ do not vanish. In addition, we perturb the scalar field,

$$\phi(r,t) = \phi(r) + \delta\phi(r,t).$$

Let us restrict ourselves to the lowest frequency modes, corresponding to spherically symmetric (or radial) perturbations, $\ell = 0$. This gives $\delta\psi = \delta\mu_3$. Then we can use the gauge freedom and fix[1]

$$\delta\psi = \delta\mu_3 \equiv 0 \Rightarrow \delta R(r, t) = 0. \tag{35}$$

Tedious calculations allow us to reduce the perturbation equations to a single wave equation

$$e^{-2\mu_2-2\nu}\delta\ddot{\phi} - \delta\phi'' - \delta\phi'(\nu' - 2\mu_3' + \mu_2') + U\delta\phi = 0, \tag{36}$$

where

$$U \equiv e^{-2\mu_2}\left(\epsilon(e^{2\mu_3} - V)\frac{(\phi')^2}{(\mu_3')^2} - \frac{2\phi'}{\mu_3'}V_{,\phi} + \epsilon V_{,\phi\phi}\right). \tag{37}$$

Introducing the new function Ψ by putting

$$\delta\phi = \Psi e^{\mu_3 + i\omega t}, \tag{38}$$

we bring the wave equation to the Schrödinger-like form

$$\frac{d^2\Psi}{dr_*^2} + (\omega^2 - V_{\rm eff}(r_*))\Psi = 0, \tag{39}$$

with the effective potential

$$V_{\rm eff} = U + \frac{1}{R}\frac{d^2R}{dr_*^2}, \tag{40}$$

$$\frac{U}{A} = \frac{\epsilon\phi'^2}{R'^2}(R^2V - 1) + \frac{2\phi' RV_{,\phi}}{R'} + \epsilon V_{,\phi,\phi}. \tag{41}$$

V. STABILITY ANALYSIS

A. Methods

Finite potentials.—If the effective potential $V_{\rm eff}$ is finite and positive-definite, the differential operator

$$W = -\frac{d^2}{dr_*^2} + V_{\rm eff} \tag{42}$$

is a positive self-adjoint operator in $L^2(r_*, dr_*)$, the space of functions satisfying proper boundary conditions. Then W has no negative eigenvalues, in other words, there are no normalizable solutions to the corresponding Schrödinger equation with well-behaved initial data (smooth data on a compact support) that grow with time, and the system under study is then stable under this particular form of perturbations. Therefore, in our stability studies, our main concern will be regions where the effective potentials are negative since possible instabilities are indicated by such regions.

The response of a stable black hole or wormhole to external perturbations is dominated at late times by a set of damped oscillations, called *quasinormal modes* (QNMs). Quasinormal frequencies do not depend on the way of their excitation but are completely determined by the parameters of the configuration itself. Thus quasinormal modes form a characteristic spectrum of proper oscillations of a black hole or a wormhole and could be called their "fingerprints". Apart from black hole physics, QNMs are studied in such areas as gauge/gravity correspondence, gravitational wave astronomy [26,27] and cosmology [28].

The quasinormal boundary conditions for black hole perturbations imply pure incoming waves at the horizon and pure outgoing waves at spatial infinity. For asymptotically flat solutions, the quasinormal boundary conditions are

$$\Psi \propto e^{\pm i\omega r_*}, \qquad r_* \rightarrow \pm\infty. \tag{43}$$

The proper oscillation frequencies correspond in a sense to a "momentary perturbation", that is, to the situation where one looks at a response of the system (say, a wormhole) to initial perturbation when the source of the perturbation stopped to act. This is the essence of the word "proper". Thus, in the wormhole case, no incoming waves are allowed coming from either of the infinities. The issue of the boundary conditions for quasinormal modes of wormholes is not completely new and was considered in [29].

Therefore, for wormholes the condition "pure incoming waves at the horizon" is replaced with "pure outgoing waves at the other spatial infinity" [29,30]. For asymptotically anti-de Sitter black holes or wormholes, the AdS boundary creates an effective confining box [26], so that on the AdS boundary one usually requires the Dirichlet boundary conditions

$$\Psi \rightarrow 0, \qquad r_* \rightarrow \infty. \tag{44}$$

This choice is not only dictated by the asymptotic of the wave equation at infinity but is also consistent with the limit of purely AdS space-time: the QNMs of an AdS black hole approach the normal modes of empty AdS space-time in the limit of a vanishing black hole radius [31]. Thus quasinormal modes of a compact object (a black hole or wormhole) in AdS space-time look like normal modes of empty AdS space-time "perturbed" by the compact object.

If the effective potential is negative in some region, growing quasinormal modes can appear in the spectrum, indicating an instability of the system under such perturbations. It turns out that some potentials with a negative gap still do not imply instability. If there are no growing quasinormal modes in the black hole or wormhole spectrum, this object is stable against linear perturbations.

Singular potentials and their regularization.—It can be seen from (40) (provided that $VR^2 < 1$) that the effective potential $V_{\rm eff}$ for radial perturbations forms an infinite wall

[1] See more details on gauges and gauge-invariant perturbations in [14,23]. The present notations are related to those in [23] as follows:

$$r \mapsto u, \qquad \nu \mapsto \gamma, \qquad R(r) \mapsto r(u),$$
$$\mu_2 \mapsto \alpha, \qquad \mu_3 \mapsto \beta.$$

located at a throat, with the generic behavior $V_{\rm eff} \sim (r - r_{\rm throat})^{-2}$, since we have there $R'(r) \sim r - r_{\rm throat}$. As a result, perturbations are independent at different sides of the throat, necessarily turn to zero at the throat itself, and we thus lose part of the information on their possible properties. To remove the divergence, one can use a method on the basis of S deformations as described in [32,33] for solutions with arbitrary potentials $V(\phi)$. For anti-Fisher wormholes ($V(\phi) \equiv 0$) it was applied in [14].

If the scalar potential $V(\phi)$ is zero, the effective potential (40) takes the form

$$V_{\rm eff}(r) = \frac{A}{R^2} - \frac{A^2 R'^2}{R^2} - \frac{\epsilon A \phi'^2}{R'^2}. \tag{45}$$

In this case the general static solution ($\omega = 0$) to Eq. (39) is

$$\Psi_0(r) = C_1 R\left(1 - \frac{\epsilon A R \phi'^2}{A' R'}\right) + \frac{C_2}{R}\left[\frac{\phi}{A'} - \frac{\epsilon A R \phi'^3}{A'^2 R'}\left(\frac{\phi}{\phi'} - \frac{2A}{A'}\right)\right], \tag{46}$$

and its special cases with $C_1 = 0$ and $C_2 = 0$ were used in [14,23] to remove the divergence in $V_{\rm eff}$. Indeed, we can introduce the new wave function

$$\bar{\Psi} = S\Psi - \frac{d\Psi}{dr_*}, \quad \text{where } S = \frac{1}{\Psi_0}\frac{d\Psi_0}{dr_*}, \tag{47}$$

which satisfies the equation

$$\frac{d^2\bar{\Psi}}{dr_*^2} + (\omega^2 - \bar{V}_{\rm eff}(r_*))\bar{\Psi} = 0 \tag{48}$$

with the effective potential

$$\bar{V}_{\rm eff} = 2S^2 - V_{\rm eff}, \tag{49}$$

and the new effective potential is everywhere regular if either $C_1 = 0$ or $C_2 = 0$. This transformation was used to prove the instability of anti-Fisher wormholes [14] and other anti-Fisher solutions [23],

It turns out that C_1 and C_2 can be both nonzero, leading to regularized effective potentials with the same quasinormal spectrum, though not preserving the symmetry $\phi \leftrightarrow -\phi$. This means that we can fix the boundary conditions arbitrarily and, if we find a "good" static solution, we can use it to remove the singularity of the effective potential.

For nonzero scalar potentials $V(\phi)$, analytical expressions for static perturbations are unknown. Therefore, such suitable solutions must be found numerically under proper boundary conditions.

First we notice that since Ψ_0 is a static solution to Eq. (39), S satisfies the Riccati equation

$$\frac{dS}{dr_*} + S^2 - V_{\rm eff} = 0. \tag{50}$$

Substituting (40) into (50), we find an expansion for S near the throat as [23]

$$S(r) = -\frac{1+c}{r} - \frac{4c^2}{3m\pi^2} + \frac{4c^2(4c^2 + (1+c)\pi^2)}{9m^2(1+c)\pi^4} r + Kr^2 + \ldots, \tag{51}$$

where K is an arbitrary constant.

With this expression we find the boundary condition for the function $S(r)$ at some points close to the throat on both sides. Then we integrate (50) numerically and find $S(r)$ between the throat and both asymptotical regions. Having $S(r)$ at hand, we find the regularized effective potential (49); it is finite at the throat due to (51).

We assigned different values to the free constant K. As a rule, we were able to integrate Eq. (50) numerically in a

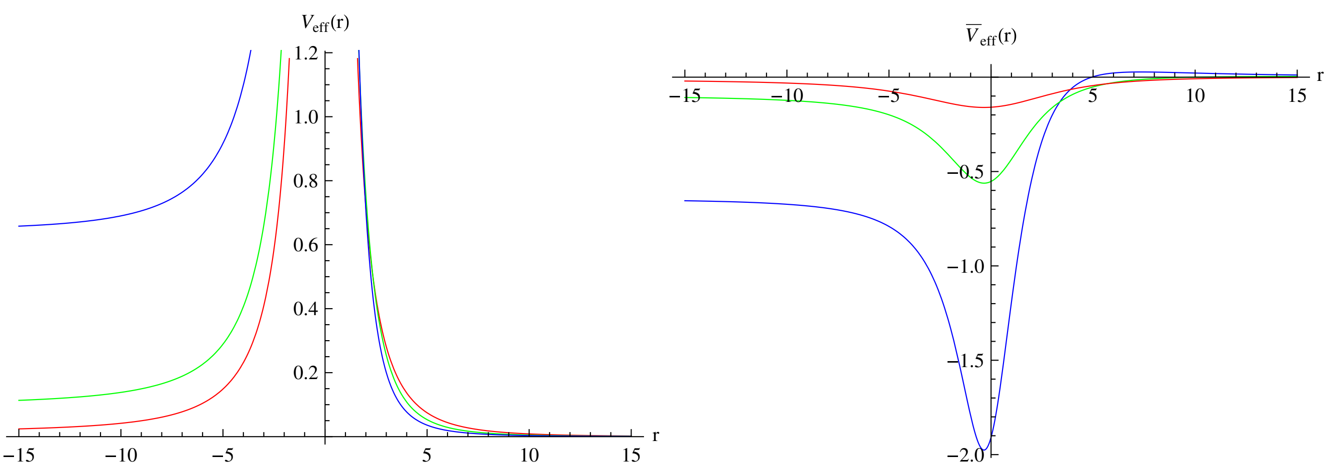

FIG. 1 (color online). Effective potentials for spherically symmetric perturbations of M-AdS wormholes with $m = -1/3$, $c = 0.3$ (red), $c = 0.5$ (green), $c = 0.8$ (blue) with divergences at the throat (left panel) and the corresponding regular ones found numerically (right panel). Larger values of c correspond to larger absolute values of $V_{\rm eff}$ at the AdS boundary (they are positive for divergent potentials and negative for regular ones).

sufficiently wide range of r near the throat. The regularized effective potentials obtained in this way always lead to the same growth rate of the perturbation function. However, for some particular values of K, the numerical integration with the Wolfram MATHEMATICA built-in function encounters a growing numerical error. Apparently, in these cases some alternative methods of integration should be used.

In addition, we used the same method to find numerically the regularized potential for the Branch B anti-Fisher solution whose stability properties had been studied previously [23]. Although the numerically found potential differs from Eq. (68) of [23], the time-domain profile again shows the same growth rate. This confirms the correctness of the method suggested and used here.

B. M-AdS wormholes with negative mass

Polar perturbations.—Now we are in a position to apply the above method to the special case of M-AdS wormholes (3) with $m < 0$, which are asymptotically AdS as $r \to -\infty$. In Fig. 1 one can see that although the initial (singular) effective potentials $V_{\rm eff}$ are positive-definite, the regularized potentials $\overline{V}_{\rm eff}$ are negative in some range around the throat and at the AdS boundary. This behavior usually indicates an instability but does not guarantee it [34]. Therefore, to prove the instability of M-AdS wormholes, we have used the time-domain integration method proposed by Gundlach *et al.* [35] and later used by a number of authors (see, e.g., [36]). The method shows a convergence of the time-domain profile with diminishing the integration grid and increasing the precision of all computations. We imposed the Dirichlet boundary conditions at the AdS boundary, as described in [37]. Figure 2 shows examples of time-domain profiles for the evolution of perturbations. The growth of the signal allows us to conclude that such wormholes are unstable against radial perturbations. At larger c we found the regularized potential with deeper negative wells and observed a quicker growth of the signal. Therefore we conclude that all such M-AdS wormholes are unstable.

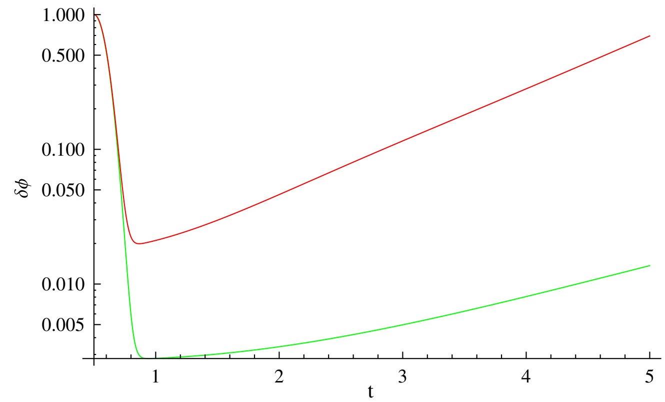

FIG. 2 (color online). Time-domain evolution of spherically symmetric perturbations of M-AdS wormholes with $m = -1/3$, $c = 0.5$ (green, bottom), and $c = 0.8$ (red, top).

Axial perturbations.—The effective potentials $V_{\rm eff}$ for axial perturbations of M-AdS wormholes $V_{\rm eff}$ are plotted in Fig. 3. One can see that above some threshold value of c, $V_{\rm eff}(r)$ has a negative gap. This threshold value of c is $c \approx 1.737$ in units for which $m = -1/3$. A further increase of c makes the negative gap deeper, however, time-domain profiles for the evolution of axial perturbations show a decay of the signal without any indication of instability (see Fig. 4).

C. Black universes

Polar perturbations.—Black universes correspond to the metric (2) and (3) with $m > 0$, $c < 0$. Black universes with $c \leq -1$, or equivalently $3\pi m \geq 2b$, have no throat in the static region. From Fig. 5 one can see that for $c = -1$ the effective potential has a negative gap, however, time-domain integration proves that in this case the black universe is stable. For smaller values of c, an additional

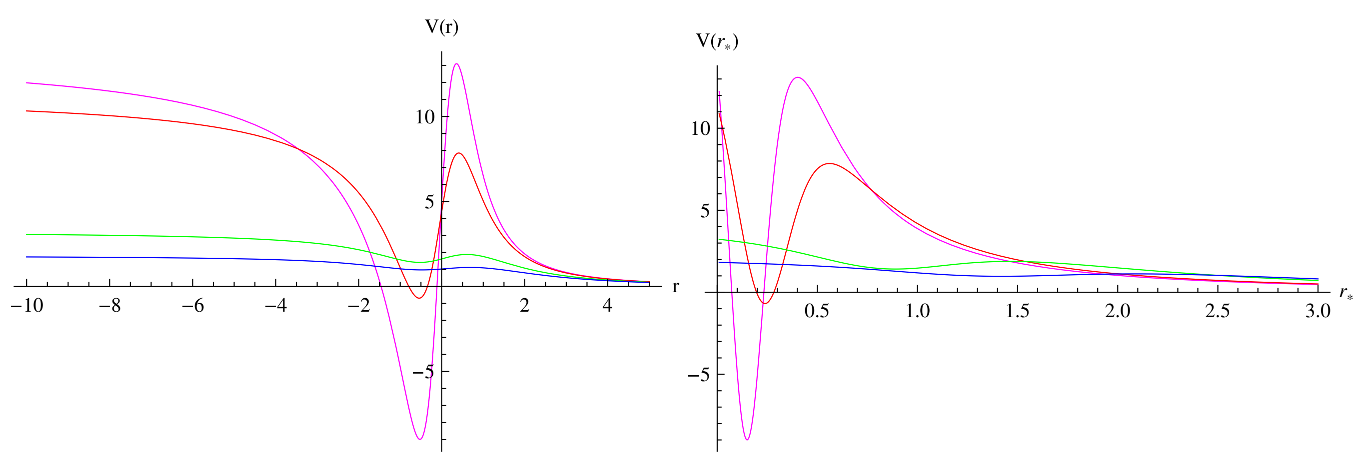

FIG. 3 (color online). Effective potential as a function of the radial coordinate r (left figure) and of the tortoise coordinate r_* (right figure) for axial gravitational perturbations of M-AdS wormholes with $m = -1/3$ for $\ell = 2$, $c = 0.8$ (no negative gap), 1.0, 1.8 (a negative gap), 2.2 (a deep negative gap).

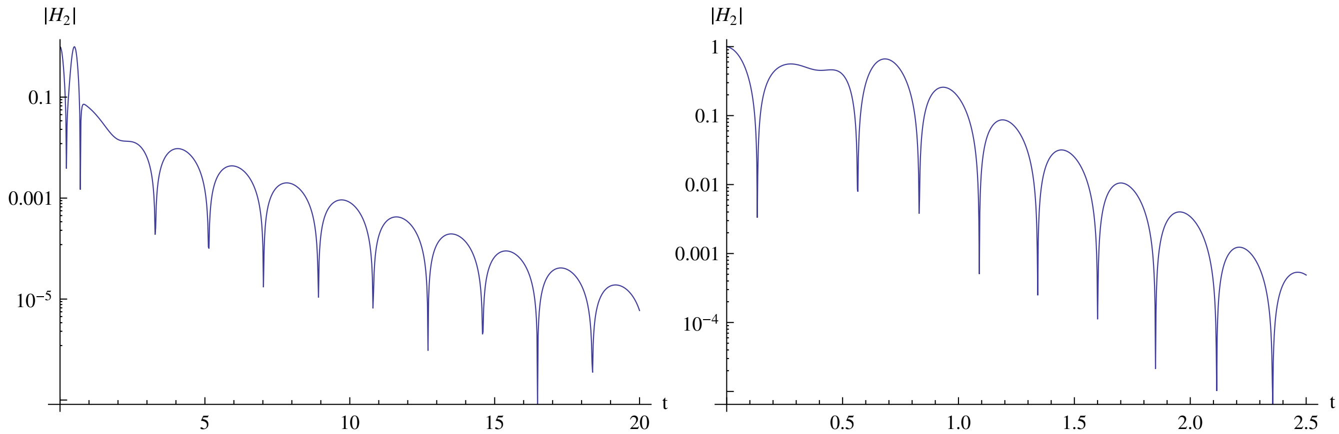

FIG. 4 (color online). Time-domain profiles of the evolution of axial ($\ell = 2$) perturbations of M-AdS wormholes ($m = -1/3$) with $c = 1$ (left) and $c = 5$ (right).

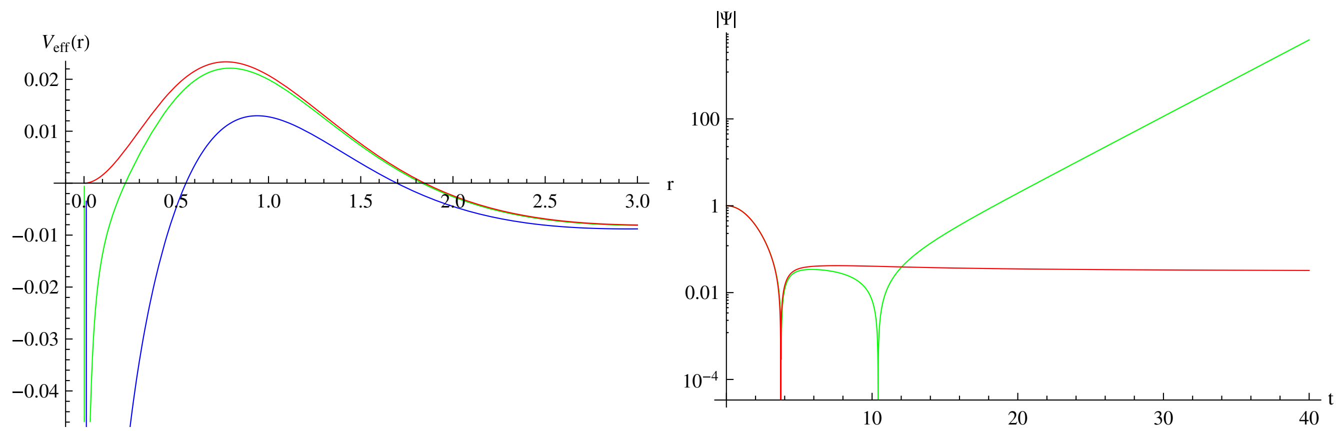

FIG. 5 (color online). Left panel: Effective potentials for radial perturbations of a black universe with $\ell = 0$, $m = 1/3$, $c = -1$ (red, top), $c = -1.001$ (green), $c = -1.01$ (blue, bottom). The potentials vanish at the horizon. Right panel: time-domain perturbation evolution for $c = -1$ (red, stable), and $c = -1.001$ (green, unstable).

negative gap appears between the peak and the horizon, leading to an instability even for $c = -1.001$. For large negative c the potential peak disappears, and the potential becomes negative everywhere (see Fig. 6), which inevitably creates an instability.

At $c > -1$ the throat $r = 0$ is in the static region. In this case we numerically find the regularized effective potentials which have large negative gaps leading to instabilities (see Figs. 7 and 8). As c approaches zero, the growth rate of time-domain profile decreases, still remaining positive because the effective potential remains negative in a wide region near the throat (Fig. 7).

As $|c|$ grows the negative gap becomes deeper and narrower, giving way to a small positive hill, which becomes broader (see Fig. 8) as c approaches -1. However, we do not observe a decrease in the growth rate as expected when approaching the parametric region of stability near $c = -1$. This can be an indication that the only parameter for which a black universe can be stable is $c = -1$.

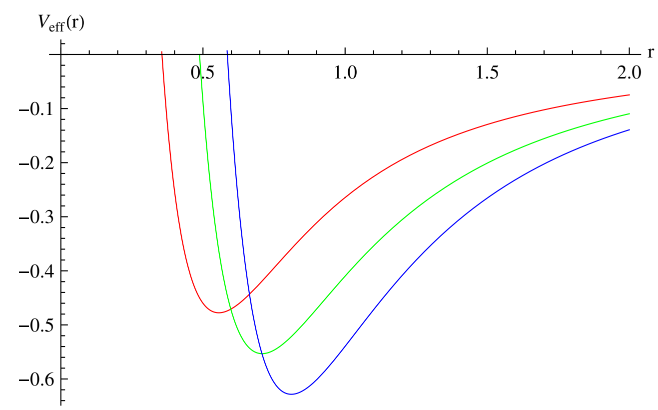

FIG. 6 (color online). Effective potential for radial perturbations of a black universe with $\ell = 0$, $m = 1/3$, $c = -1.5$ (red, top), $c = -2$ (green), $c = -3$ (blue, bottom). The potentials vanish at the horizon.

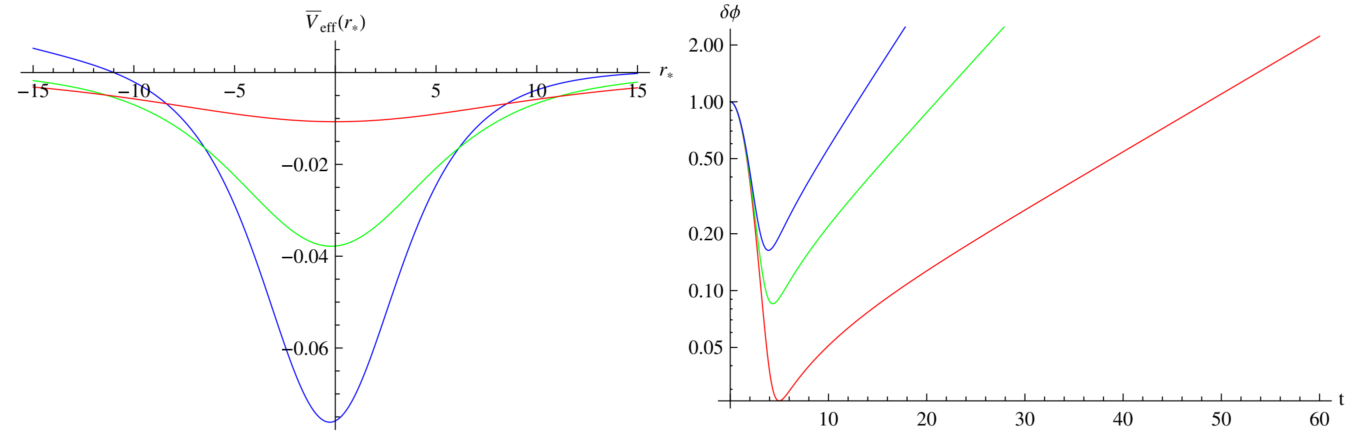

FIG. 7 (color online). Regularized effective potentials (left panel, top to bottom) and time-domain profiles (right panel, bottom to top) for radial perturbations of a black universe with $\ell = 0$, $m = 1/3$, $c = -0.1$ (red), -0.2 (green), -0.3 (blue).

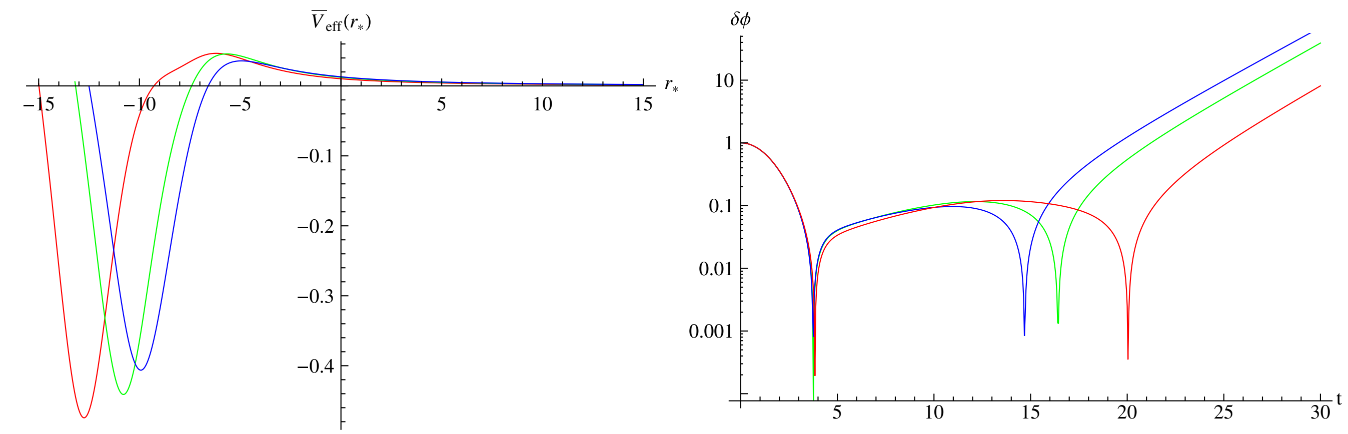

FIG. 8 (color online). Regularized effective potentials (left panel) and time-domain profiles (right panel) for radial perturbations of a black universe with $\ell = 0$, $m = 1/3$, $c = -0.90$ (blue), -0.95 (green), -0.99 (red). Larger negative values of c correspond to deeper negative gaps and later growing phase of the signal.

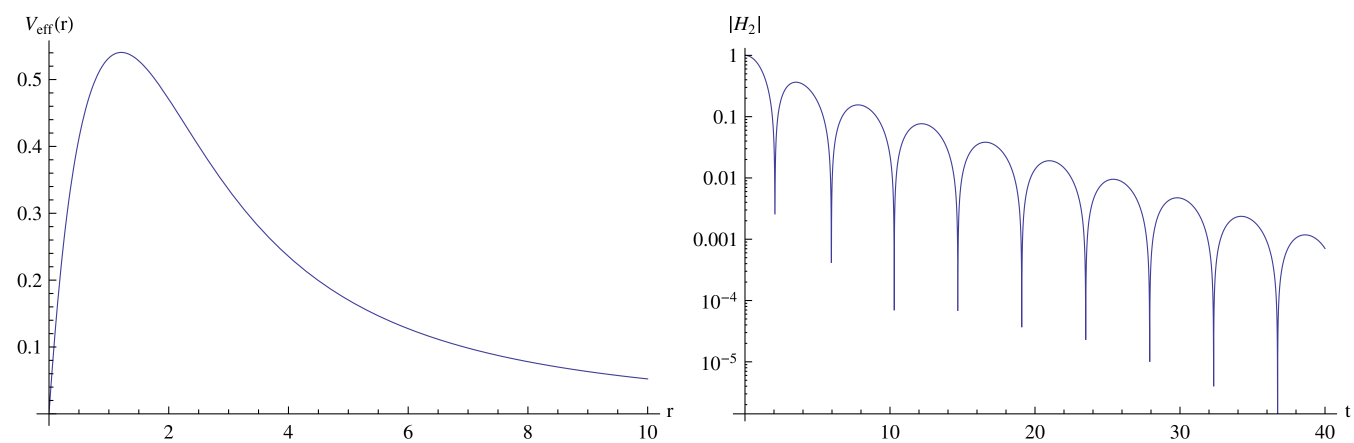

FIG. 9 (color online). The effective potential (left panel) and the time-domain profile (right panel) for axial gravitational perturbations of black universes for $\ell = 2$, $m = 1/3$, $c = -1$. The potential vanishes at the horizon $r = 0$.

Axial perturbations and quasinormal oscillation frequencies.—From Fig. 9 we can see that in the static region the effective potential is positive-definite. Therefore, if we perturb a black hole "on the right" of the event horizon (Fig. 9), such perturbations are stable. Beyond the event horizon, in the cosmological region, the effective potential can take large negative values, but this has no effect on perturbations propagating outside the horizon. We therefore conclude that the black universes under consideration are stable against axial perturbations in the static region.

As we have shown, black universes at $c = -1$ ($b = 3\pi m/2$) are stable against polar monopole perturbations, and their response to external perturbations is dominated at late times by the quasinormal (QN) frequencies. Supposing $\Psi \propto e^{-i\omega t}$, quasinormal modes can be written in the form

$$\omega = \omega_{\rm Re} - i\omega_{\rm Im},$$

where a positive $\omega_{\rm Im}$ is proportional to the decay rate of a damped QN mode. The low-lying axial QN frequencies have the smallest decay rates in the spectrum and thus dominate in a signal at sufficiently late times. They can be calculated with the help of the WKB approach [38,39].

Introducing $Q = \omega^2 - V_{\rm eff}$, the sixth order WKB formula reads

$$\frac{iQ_0}{\sqrt{2Q_0''}} - \sum_{k=2}^{6}\Lambda_k = n + \frac{1}{2}, \qquad n = 0, 1, 2\ldots, \tag{52}$$

where the correction terms Λ_k were obtained in [38,39]. Here Q_0 and Q_0^k are the value and the kth derivative of Q at its maximum with respect to the tortoise coordinate r_*, and n labels the overtones. The WKB formula (52) was effectively used in a lot of papers (see, e.g., [40] and references therein).

The WKB formula gives an accurate result for large multipole numbers (see Table I). Expanding the WKB formula it powers of ℓ, we find the following asymptotical expression for $c = -1$:

$$\omega b = \sqrt{\frac{2}{\pi}\tan^{-1}\left(\frac{2}{\pi}\right)}\left(\ell + \frac{1}{2} - i\left(n + \frac{1}{2}\right)\right) + \mathcal{O}\left(\frac{1}{\ell}\right).$$

In Table I, the asymptotic formula for the fundamental mode (the one that dominates at late times) is presented in units $m = 1/3$, so that $b = \pi/2$.

TABLE I. Quasinormal modes of axial perturbations of black universes with $c = -1$ ($m = 1/3$).

ℓ	WKB6	Time-domain fit
2		$0.712299 - 0.157848i$
3	$1.168844 - 0.176095i$	$1.169144 - 0.176019i$
4	$1.590954 - 0.182539i$	$1.590956 - 0.182542i$
5	$1.997792 - 0.185591i$	$1.997801 - 0.185588i$
$\gg 1$	$0.191226(2\ell + 1 - i)$	

The WKB formula (52) used here is developed for effective potentials which have the form of a barrier with only one peak (see, e.g., Fig. 9 for black universes), so that there are two turning points given by the equation $\omega^2 - V_{\rm eff} = 0$. Therefore, it cannot be used for effective potentials which have negative gaps, that is, for testing the stability of all questionable cases.

VI. CONCLUSIONS

We have developed a general formalism for analyzing axial gravitational perturbations of an arbitrary static, spherically symmetric solution to the Einstein-Maxwell-scalar equations where the scalar field, which can be both normal and phantom, is minimally coupled to gravity and possesses an arbitrary potential. This can be used for studying the stability and QNM modes of diverse charged and neutral scalar field configurations in general relativity. As to polar perturbations, we have restricted ourselves to the monopole mode, i.e., to spherically symmetric (radial, for short) perturbations.

We have applied this formalism to some electrically neutral wormholes and black holes supported by a phantom scalar field. The main results which were obtained here are:

(1) M-AdS wormholes described by the solution (3) with negative mass are shown to be unstable under radial perturbations, although the initial effective potential with a singularity at the throat is positive everywhere. These features are similar to those of anti-Fisher wormholes [14] which are twice asymptotically flat.

(2) Black universes (i.e., regular black holes with de Sitter expansion far beyond the horizon), described by the solution (3) without throats in the static region, are shown to be stable only in the special case where the horizon coincides with the minimum of the area function $R(r)$ (the parameters: $c = -1$, $b = 3\pi m/2$) and unstable for $c \neq -1$.

(3) Quasinormal modes of axial perturbations have been calculated for stable black universes.

Quite a lot of other problems of interest are yet to be studied. One can mention a full nonlinear analysis of perturbations in all relevant cases. Next, the formalism developed here for linear perturbations allows us to include the electromagnetic field into consideration and study charged solutions with both normal and phantom scalar fields. Last but not least, using the well-known conformal mappings that relate Einstein and Jordan frames of scalar-tensor and curvature-nonlinear theories of gravity, one can extend the studies to solutions of these theories.

ACKNOWLEDGMENTS

The work of K. B. was supported in part by RFBR Grant No. 09-02-00677a, by NPK MU Grant at PFUR, and by FTsP "Nauchnye i nauchno-pedagogicheskie kadry innovatsionnoy Rossii" for the years 2009–2013. R. K.

acknowledges the Centro de Estudios Cientifcos (Valdivia, Chile) where part of this work was done. At its initial stage the work was partially funded by the Conicyt Grant No. ACT-91: "Southern Theoretical Physics Laboratory" (STPLab). The Centro de Estudios Cientifcos (CECS) is funded by the Chilean Government through the Centers of Excellence Base Financing Program of Conicyt. At the final stage R. K. was supported by the European Commission Grant through the Marie Curie International Incoming Contract. A. Z. was supported by Deutscher Academischer Austausch Dienst (DAAD) and Conselho Nacional de Desenvolvimento Científico e Tecnológico (CNPq).

[1] N. A. Bahcall, J. P. Ostriker, S. Perlmutter, and P. J. Steinhardt, Science **284**, 1481 (1999); S. J. Perlmutter *et al.*, Astrophys. J. **517**, 565 (1999); V. Sahni and A. A. Starobinsky, Int. J. Mod. Phys. A **9**, 373 (2000).
[2] E. Komatsu, Astrophys. J. Suppl. Ser. **192**, 18 (2011).
[3] M. Sullivan *et al.*, Astrophys. J. **737**, 102 (2011).
[4] R. Gannouji, D. Polarski, A. Ranquet, and A. A. Starobinsky, J. Cosmol. Astropart. Phys. 09 (2006) 016; A. Vikman, Phys. Rev. D **71**, 023515 (2005); R. R. Caldwell, M. Kamionkowski, and N. N. Weinberg, Phys. Rev. Lett. **91**, 071301 (2003); S. Chattopadhyay and U. Debnath, Braz. J. Phys. **39**, 86 (2009); Z.-Y. Sun and Y.-G. Shen, Gen. Relativ. Gravit. **37**, 243 (2005); L. P. Chimento and R. Lazkoz, Phys. Rev. Lett. **91**, 211301 (2003).
[5] M. Jamil and M. U. Farooq, Int. J. Theor. Phys. **49**, 835 (2010); V. Dzhunushaliev, V. Folomeev, R. Myrzakulov, and D. Singleton, J. High Energy Phys. 07 (2008) 094; S. V. Sushkov, Phys. Rev. D **71**, 043520 (2005); J. A. Gonzalez and F. S. Guzman, Phys. Rev. D **79**, 121501 (2009); F. S. N. Lobo, Phys. Rev. D **71**, 084011 (2005); D. Ida and S. A. Hayward, Phys. Lett. A **260**, 175 (1999).
[6] K. A. Bronnikov and G. N. Shikin, Gravitation Cosmol. **8**, 107 (2002); U. Nucamendi and M. Salgado, Phys. Rev. D **68**, 044026 (2003); O. Bechmann and O. Lechtenfeld, Classical Quantum Gravity **12**, 1473 (1995).
[7] H. Ellis, J. Math. Phys. (N.Y.) **14**, 104 (1973).
[8] K. A. Bronnikov, Acta Phys. Pol. B **4**, 251 (1973).
[9] K. A. Bronnikov and J. C. Fabris, Phys. Rev. Lett. **96**, 251101 (2006).
[10] K. A. Bronnikov, H. Dehnen, and V. N. Melnikov, Gen. Relativ. Gravit. **39**, 973 (2007).
[11] K. A. Bronnikov and E. V. Donskoy, Gravitation Cosmol. **16**, 42 (2010).
[12] K. A. Bronnikov and S. V. Sushkov, Classical Quantum Gravity **27**, 095022 (2010).
[13] K. A. Bronnikov and E. V. Donskoy, Gravitation Cosmol. **17**, 176 (2011).
[14] J. A. Gonzalez, F. S. Guzman, and O. Sarbach, Classical Quantum Gravity **26**, 015010 (2009).
[15] H.-a. Shinkai and S. A. Hayward, Phys. Rev. D **66**, 044005 (2002).
[16] J. A. Gonzalez, F. S. Guzman, and O. Sarbach, Classical Quantum Gravity **26**, 015011 (2009).
[17] A. Doroshkevich, J. Hansen, I. Novikov, and A. Shatskiy, Int. J. Mod. Phys. D **18**, 1665 (2009).
[18] C. Armendariz-Picon, Phys. Rev. D **65**, 104010 (2002).
[19] I. Z. Fisher, Zh. Eksp. Teor. Fiz. **18**, 636 (1948); arXiv:gr-qc/9911008.
[20] O. Bergmann and R. Leipnik, Phys. Rev. **107**, 1157 (1957).
[21] K. A. Bronnikov, M. S. Chernakova, J. C. Fabris, N. Pinto-Neto, and M. E. Rodrigues, Int. J. Mod. Phys. D **17**, 25 (2008).
[22] K. A. Bronnikov and A. V. Khodunov, Gen. Relativ. Gravit. **11**, 13 (1979).
[23] K. A. Bronnikov, J. C. Fabris, and A. Zhidenko, Eur. Phys. J. C **71**, 1791 (2011).
[24] S. Chandrasekhar, *The Mathematical Theory of Black Holes* (Clarendon Press, Oxford, 1983).
[25] H. Dennhardt and O. Lechtenfeld, Int. J. Mod. Phys. A **13**, 741 (1998).
[26] R. A. Konoplya and A. Zhidenko, Rev. Mod. Phys. **83**, 793 (2011).
[27] K. D. Kokkotas and B. G. Schmidt, Living Rev. Relativity **2**, 2 (1999).
[28] W. A. Hiscock, Phys. Rev. D **17**, 1497 (1978); S. N. Guha Thakurta, Phys. Rev. D **21**, 864 (1980); R. A. Konoplya, Phys. Lett. B **706**, 451 (2012); R. A. Konoplya and A. Zhidenko, arXiv:1110.2015.
[29] R. A. Konoplya and C. Molina, Phys. Rev. D **71**, 124009 (2005).
[30] R. A. Konoplya and A. Zhidenko, Phys. Rev. D **81**, 124036 (2010).
[31] R. A. Konoplya, Phys. Rev. D **66**, 044009 (2002).
[32] M. S. Volkov and D. V. Gal'tsov, Phys. Rep. **319**, 1 (1999).
[33] H. Kodama and A. Ishibashi, Prog. Theor. Phys. **111**, 29 (2004).
[34] R. A. Konoplya and A. Zhidenko, Phys. Rev. D **78**, 104017 (2008).
[35] C. Gundlach, R. Price, and J. Pullin, Phys. Rev. D **49**, 883 (1994).
[36] J. Morgan, V. Cardoso, A. S. Miranda, C. Molina, and V. T. Zanchin, J. High Energy Phys. 09 (2009) 117; R. A. Konoplya and A. Zhidenko, Phys. Rev. Lett. **103**, 161101 (2009); R. A. Konoplya and C. Molina, Phys. Rev. D **75**, 084004 (2007).
[37] B. Wang, C. Molina, and E. Abdalla, Phys. Rev. D **63**, 084001 (2001).
[38] B. F. Schutz and C. M. Will Astrophys. J. Lett. **291**, L33 (1985); S. Iyer and C. M. Will, Phys. Rev. D **35**, 3621 (1987).
[39] R. A. Konoplya, Phys. Rev. D **68**, 024018 (2003); J. Phys. Stud. **8**, 93 (2004).
[40] H. Kodama, R. A. Konoplya, and A. Zhidenko, Phys. Rev. D **81**, 044007 (2010); R. A. Konoplya and A. Zhidenko, Phys. Lett. B **644**, 186 (2007); O. P. F. Piedra and J. de Oliveira, Classical Quantum Gravity **28**, 085023 (2011); K. Lin, N. Yang, and J. Li, Int. J. Theor. Phys. **50**, 48 (2011).